Nonlinear Behavior of Pile-Soil Subjected to Torsion due to Environmental Loads on Jacket Type Platforms

M.R. EMAMI AZADI, Assistant Professor,
Department of Civil Eng., Azarbaijan T.M. University, Tabriz IRAN
dr.emami@azaruniv.edu

and

S. NORDAL, Professor,
Department of Geotechnical Eng., Univ. of Science & Technology, NORWAY
s.nordal@hotmail.com

and

M.SADEIN, M.Sc. Student
Department of Civil Eng., Univ. of Tabriz, Tabriz, IRAN
msadein@yahoo.com

Abstract: - In the present study, the torque-twist behavior of non-linear pile-soil system related to the wave-current loading on Jacket type offshore platform is investigated. The non-linearities of pile-soil with respect to both depth and the twist angle of pile are considered. The basic differential equilibrium equations of the pile-soil system are derived based on hyper- elasticity theory of soil. A numerical central finite difference method is applied based on simplification of stress field around the pile elements which takes into account changes in the secondary shear stress components and also non-linearities due to non-homogeneous soil condition. This method uses a one-dimensional mesh along pile-soil interface. It also takes into account the changes in G of soil with respect to the twist angle of pile. In a separate work, the simulated torque-twist behavior of pile-soil system based on this analysis approach is compared with the results of more refined finite element analysis by using continuum mechanics theory and also full scale pile-soil test results (Emami,2002). The torque-twist results by using the proposed approach have been used to study the behavior of two jacket-pile-soil systems under sea environmental and accidental loading.

Key-Words: - Pile-Soil interaction, Jacket-Pile-Soil system, Pile-Soil Non-linearities, Disk Model of Soil, Torque-Twist (t-t) transfer curves

1 Introduction

In the recent years, the integrated analysis of Jacket-pile-soil systems has been one of the main concerns of the offshore industry. In this regard, modeling of pile-soil interaction has become an important issue. Therefore, most efforts in the past three decades have been put into modeling the pile-soil interaction under axial and lateral loading.

In the existing API code for offshore pile design, the so-called t-z, q-z and p-y curves are applied to simulate the non-linear pile-soil interaction behavior under axial and lateral loading, respectively. However, the recent studies show that the torque-twist interaction of pile-soil system in some cases can not be neglected. Hence, there is a need for such effect which could be considered with a torque-twist (t-t) type curve similar to t-z, q-z and p-y curves as described in API RP2A.

The topic of torsional pile-soil interaction has been focus of only few studies in the recent decades. However, the elastic pile-soil interaction behavior has been initially studied by well-known authors such as Poulos(1975) and Randolph(1982) and Stoll(1976) .Randolph(1982) investigated the torque-twist behavior of rigid piles as well as elastic flexible piles.

Poulos(1975) made a linear elastic pile-soil assumption based on continuum mechanics approach and applied boundary integral equation technique to obtain charts for pile's torsional flexibility as a function of pile's geometry and relative stiffness .While Randolph in his pioneering work, applied theory of elasticity to obtain the differential equation for the torsional pile-soil interaction. He used a rather simple stress field assumption around single pile and obtained closed forms for his analytical solutions. Stoll (1976) in his semi- analytical method used the pile-soil torque-twist data to back-figure the shear modulus of soil (G). Then he showed that it might be more economic and also rather accurate to use twist data from pile tests to predict the axial behavior of pile-soil system instead of performing more costly axial large diameter pile tests.

In the most recent work, Manuel and Gladys(2002) has proposed a quite simple strength of material based method to simulate the behavior of pile foundation under torsion. He did not elaborate further and nor mentioned the results of application of such method. His proposition was based on the assumption of virtual fixity of pile foundation at a certain depth.

In the present study, a set of torque-twist (t-t) interaction curves similar to the pile-soil axial and lateral interaction curves (t-z), (q-z) and (p-y) are developed based on disk soil discrete element approach (see Emami, 1998).

2 Theoretical Backgrounds

The idea of finite disk or strip idealization of soil medium around the pile has been introduced in the recent years by several authors such as Grande and Nordal(1979), Nogami and Konagai(1989), Wolf and Meek(1992) and Svano et al.(1993). The concept is based on idealization of pile-soil interaction as finite uncoupled circular disks as illustrated in Fig.1. Various forms of soil disks have been used so far such as rigid, elastic deformable and elasto-plastic disks.

In this work a new (t-t) model is introduced which is developed based on the idealization of the pile-soil system by a set of uncoupled imaginary finite disks. Each disk as shown in Fig.1 represents the torsional interaction between the pile and its surrounding soil. This new model is an extension of (t-z) type disk model by Grande and Nordal (1979) and Nordal et al. (1985) for torque-twist problem. Also in this new model, a tangent stiffness formulation is used instead of secant stiffness as applied in the previous model. The maximum mobilized shear stress induced due to applied torque at the pile-soil interface is determined based on Mohr-Coulomb theory. This approach is rather simple but different from the previous model. The applied torque in the pile due to environmental or even accidental loading on the jacket platform is carried and distributed through these imaginary disks to the ground. The induced shear stresses may be assumed to vary exponentially towards zero at the edges of the each disk. Plane strain conditions are assumed over each pile-soil disk (i.e. strain components assumed to be constant through the disk thickness).

The soil condition is assumed to be un-drained (clay) under short term loading hence its volume could be considered as constant after undergoing shear deformations. The radius of each finite disk (r_{id}) is assumed to be (η) times the radius of the pile (r). Here (η) may be chosen to be in the range of 10-20 to be sufficient for approximation of shear strain distribution in the soil. From simple continuum mechanics, the shear strain of the pile-soil (γ) may be calculated as follows:

$$\gamma_{r\theta} = \int_{\tau_0}^{\tau} \frac{d\tau_{r\theta}}{G^T} \tag{1}$$

where ($\tau_{r\theta}$) is the shear stress induced by torque around the pile and (G^T) is the tangent shear modulus of the soil which may be calculated from the following empirical relationship obtained by Lango(1991) through series of triaxial tests on clay:

$$G^t = G_i[1-\alpha.\frac{\tau_{r\theta}}{(\tau_{r\theta})_{ps}}]^{\beta} \tag{2}$$

Where (G_i) is the initial shear modulus of the soil, (α) and (β) are the material parameters found by Svano et al. (1993) for various soil types. The practical range of (β) is between 1 and 4. Equivalent values of β can be found for sand type soils (see Emami, 1998). In Eq.2 $(\tau_{r\theta})_{ps}$ denotes the pile-soil interface shear stress at failure. If we take an exponential form distribution for τ over the imaginary disk radius as:

$$\tau_{r\theta} = \tau_i \exp(\frac{r_i - r}{2r_i}) \tag{3}$$

Combining, the Esq. (1) to (3) and integrating Eq. (1) above may lead to:

$$\gamma = \frac{\tau}{G_i\alpha(1-\beta)}[1-(1-\alpha\frac{\tau_i}{\tau_{ps}}\exp(\frac{r_i - r}{2r_i})^{1-\beta}] \tag{4}$$

The angle of twist (φ) may then be computed as follows:

$$\varphi_t = \int_{r_i}^{r_{id}} \frac{\gamma_{r\theta}}{r} .dr \tag{5}$$

Subsequently from simple continuum mechanics theory, we can compute the corresponding torque (T) as follows:

$$T = \int_{z_i}^{z_{i+1}} 2\pi r_i^{\,2} (\tau_{r\theta})_i .dz \tag{6}$$

From Eq. (6) by assuming different values for $(\tau_{r\theta})$i, T for the given segment of pile may be obtained. While the corresponding angle of twist (φ) at the pile-soil interface can also be found. A set of t-φ values can then be computed which will characterize the so-called (t-t) pile-soil interaction curves. A verification study of (t-t) model presented here which includes comparison with other methods and also experimental results, is performed and given in a separate report by Emami(2002). The (t-t) curves are then used for integrated jacket-pile-soil analysis (see Moan et al.1997 and Emami, 1998).

2.2 Elasto-Plastic Modeling of Pile-Soil Springs

A general elasto-plasticity model for a one node spring has been implemented into usfos program (see e.g. Emami, 1998). This model is used here with the load-transfer displacement characteristic curves such as (t-z), (p-y), (q-z) and (t-t) as described in the previous subsection. The main features of the model may be outlined as:

. Plasticity model includes an isotropic type hardening/softening which implies that the extension or contraction of the yield surface is allowed.

. Hardening or softening may be associated with the presented disk for axial and lateral loading of pile-soil system.

. The model accounts for the change in the loading direction in the XY plane by means of an interaction surface.

. No scaling of load step due to plastification of the pile-soil interaction element is performed.

. No coupling is allowed between the various load

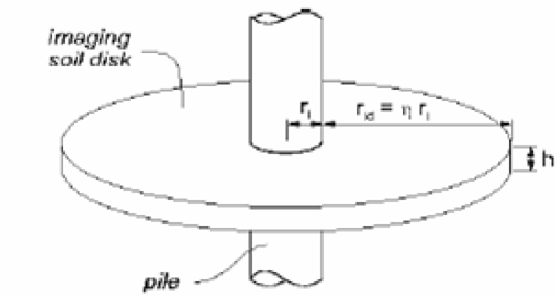

Fig.1 Disk Idealization of Pile-Soil System

transfer-displacement curves related to the pile-soil disk.

2.2.1 Pile-Soil Element Formulation

One node finite element equivalent to the pile-soil interaction disk is considered with 6DOFs as follows (see e.g. Emami, 1998):

$$\mathbf{U=[w\ \ \Phi]} \tag{7}$$

Where, w and $\mathbf{\Phi}$ represent the sub-vectors of the translational and rotational degrees of freedom. Often the rotational degrees of freedom are set to zero and hence $\mathbf{k_e}$ reduces to 3x3 but in this work we have also considered the pile-soil torsional stiffness term in the elastic stiffness matrix of pile-soil disk element. To compute the plastic stiffness matrix, we considered generalized strains/displacements as follows:

$$u = \phi^T q \tag{8}$$

Then, we have:

$$S = \phi^T Q \tag{9}$$

Decomposing the incremental displacement into elastic and plastic parts, we can write:

$$du = du_e + du_p \tag{10}$$

The corresponding elastic force-displacement relationship can be expressed as follows:

$$dS = k_e du_e \tag{11}$$

The corresponding plastic strain rate relationship can then be written according to the normality rule as:

$$du_p = d\lambda . \frac{\partial F}{\partial S} \tag{12}$$

The isotropic hardening rule can then be applied as follows:

$$dR = H_R.d\lambda \tag{13}$$

The yield condition can then expressed as follows:

$$\Gamma = \left|S - X\right| - R(u_p) = 0 \tag{14}$$

The gradient to the yield surface can then computed as follows:

$$g = \frac{\partial F}{\partial S} \tag{15}$$

And also:

$$g_R = \frac{\partial F}{\partial R} \tag{16}$$

The elasto-plastic stiffness of the pile-soil disk element can then established applying the consistency condition as follows:

$$\Delta F = \frac{\partial F}{\partial S}.dS + \frac{\partial F}{\partial R}.dR \tag{17}$$

Combining the above equations, we get the following matrix relationship:

$$g^T.K_e(du - gd\lambda) + g_R.H_R.d\lambda = 0 \tag{18}$$

Hence, we can obtain the increment of scaling factor as:

$$d\lambda = (g^T.K_e.g - g_R.H_R)^{-1}.g^T.K_e.du \tag{19}$$

Using the above Equations, we might obtain the following elasto-plastic stiffness relationship for the pile-soil interaction disk:

$$dS = K_{ep}.du = K_e(du - du_p = g.d\lambda) \tag{20}$$

Where substituting in Eq.20 for $d\lambda$ from Eq.19 above, we shall obtain:

$$dS = [K_e - K_e.g(g^T.K_e.g - g_R.H_R)^{-1}.g^T.K_e].du \tag{21}$$

Eq.21 shows that the elasto-plastic stiffness of the pile-soil interaction disk in this case is a function of non-linear elastic (hyper-elastic= K_e) stiffness, gradient (g) and isotropic type plastic hardening function of the pile-soil disk (H_R).

2.2.2 Jacket-Pile-Soil System Stiffness Formulation

The computed structural and pile-soil disk element stiffness matrices are transformed from local to a global coordinate system as follows:

$$K^i_{ep,gl} = \psi^T{}_i K^i_{ep} \psi_i \tag{22}$$

Where ψ_i indicate the vector of cosine directions for each element (**i**) in the above equation (see for e.g. Perzemienicki,1968 and Zienkiewich,1989).

The transformed element stiffness matrices then are assembled in a global stiffness matrix as:

$$K_r = \sum_{i=1}^{n} A_i^T.K^i_{ep,gl}.A_i \tag{23}$$

In which A_i is a system stiffness transformation matrix, relating the element Dofs into global coordinate system (see for e.g. Perzemieniecki, 1968 and Reddy, 1989). Alternatively, a superposition approach may be adopted to transform the element stiffness matrices into the system stiffness matrix K_r .

K_r can then be updated after each incremental step.

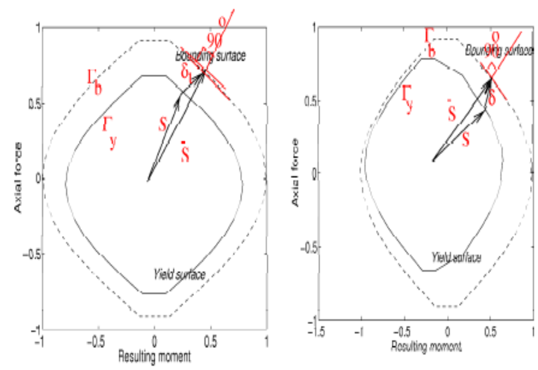

Fig.2 Double Bounding yield surface concept

2.2.3 Plasticity Formulation for Structural Members

The normality rule on structural element can be expressed as follows (see Soreide et al,(1986)) :

$$\delta v_p = G_u.\Delta\lambda = [g_i]^T.\Delta\lambda \tag{24}$$

In which, δv_p represents the incremental plastic displacement vector at structural element level. The **[gi]** denotes the gradient matrix on the right-hand-side of Eq.24 which is also multiplied by scaling increment. The **g_i** elements represent the Green function of structural beam member used to model the Jacket and Piles which can be computed as:

$$g_i{}^T = \frac{\partial \Gamma}{\partial S_i} \tag{25}$$

Where, Γ denotes the plastic interaction function for the structural beam element as shown in Fig.2 below. S_i refers to the general force vector at the node (i) of beam element. For the tubular jacket steel members the following plastic interaction formula was given by Soreide et al, (1986):

$$\Gamma = Cos(\frac{\pi}{2}.\frac{N}{N_p}) - \sqrt{\frac{M_y^{\,2} + M_z^{\,2}}{M_p^{\,2}}} = 0 \qquad (26)$$

In which N, N_P, M_y, M_z *and* M_p denote the axial force, plastic axial force , the bending moments about z and y axes and the plastic moment of the beam element, respectively.

A kinematic hardening rule is applied at element plasticity level in accordance with a two layer bounding surface system. Hence, the transition from the initial yield surface to the full yield state can be achieved by translation of the inner yield surface towards the outer surface in a unidirectional manner.

The stiffness matrix for the structural member may be written as follows:

$$\Delta S = K^T.\Delta v_e \qquad (27)$$

Where K^T and Δv_e denote the tangent stiffness and the elastic displacement increment, respectively. The latter can be written in the following manner:

$$\Delta v_e = \Delta v - \Delta v_p \qquad (28)$$

Combining Eqs.27 and 28 above might yield the following incremental force-displacement relationship:

$$\Delta S = K^T.(\Delta v - G_u.\Delta\lambda) \qquad (29)$$

The consistency rule requires that the force vector during the yield has to remain on the yield surface, that is to say:

$$\Delta\Gamma = \frac{\partial\Gamma}{\partial S}.\Delta S = G_u^{\,T}.\Delta S = 0 \qquad (30)$$

Substituting for ΔS in Eq.30 from R-H-S of Eq.29, we can obtain the following relationship:

$$\Delta\Gamma = G_u^{\,T}.\Delta S = G_u^{\,T} K^T.(\Delta v - G_u.\Delta\lambda) \qquad (31)$$

Then $\Delta\lambda$ can be computed from Eq.31 as follows:

$$\Delta\lambda = (G_u^{\,T}.K^T.G_u)^{-1}.(G_u^{\,T}.K^T.\Delta v) \qquad (32)$$

Replacing for $\Delta\lambda$ now in Eq.29, will yield the following elasto-plastic stiffness relationship:

$$\begin{aligned}\Delta S &= [K^T - G_u(G_u^{\,T}K^TG_u)^{-1}G_u^{\,T}K^T]\Delta v \\ &= K_{ep}.\Delta v\end{aligned} \qquad (33)$$

2.2.4 Solution Procedure

The solution procedure can be adopted to solve the problem is an iterative-incremental one. The nonlinear dynamic equation of motion of the vessel impact on the jacket platform is integrated in the time domain by means of HHT-α algorithms (Hilber et al, 1976). This algorithm is actually based on the Newmark's-β family of schemes, however, it introduces some numerical damping by means of time averaging. The dynamic incremental equilibrium equation then reads:

$$\begin{aligned}&(M + M_a)\ddot{r}_{n+1} + (1+\alpha)C(r)\dot{r}_{n+1} - \alpha C(r)\dot{r}_n + \\ &(1+\alpha)K(r)r_{n+1} - \alpha K(r)r_n = (1+\alpha)F_{e,n+1} - \alpha F_{e,n}\end{aligned} \qquad (34)$$

Where, **n** and **n+1** denote two consecutive time states. The effect of α parameter is to damp out higher order frequency contributions into the global platform response. ***M, M_a, C(r)*** and ***K(r)*** represent the structural mass matrix, the hydrodynamic added mass matrix, the damping matrix and the restoring force matrix, respectively. The numerical integration of *Eq.5* can be performed by means of a conventional predictor-corrector scheme. This method allows for time-step scaling in the predictor phase in order to bring the force status back to the yield surface.

3 Case Studies

The presented model above is applied for integrated static and dynamic analyses of two Jacket platforms, a 4-leg Malaysian Jacket and an 8-leg North-sea Jacket, respectively. The description of structural and foundation system of these two platforms are given in more detail by Emami (1998).

3.1 Case 1: A 4-leg Malaysian Jacket

3.1.1 Structural System

The structure is a light 4-leg Jacket installed in shallow waters offshore Malaysia. The finite element model of the Jacket and its 4 single pile foundation is shown in Fig.3. The bracing system of the jacket comprises only cross X-type bracing. The deck supporting module has been modeled by an additional light frame at the top of the jacket with a height of about 7.5m above mean water level. The Jacket-pile connections have not been modeled.

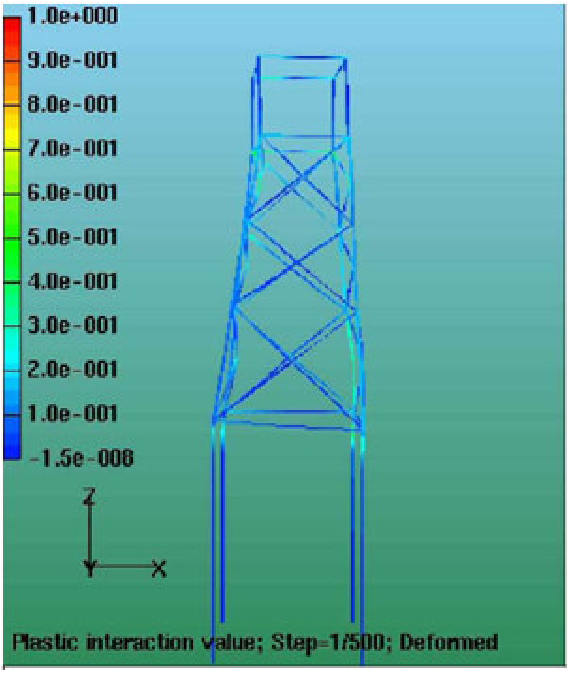

Fig.3 FE Model of 4-Leg Jacket-Pile-Soil system

3.1.2 Foundation System

The foundation of the Jacket as described above consists of 4 single vertical piles driven through the soil layers as shown in Fig.3. The piles are made of steel tubular sections with a yield strength of 470MPa which are driven into a depth of about 45m. The soil condition here is virtually varied in order to perform a sensitivity study on the influence of (p-y) curves as well as (t-t) curves stiffness and capacities. The piles here are supposed to be un-plugged initially. However, during the parametric studies the piles in some cases are supposed to be supported on their tips. The detail description of soil layers is given in Emami (1998).

3.1.3 Load Description

The load vector consists of gravity, wave and current induced components. However, to investigate the influence of the torque (torsion moment) on the behavior of piles and the whole platform, it is assumed that a large part of structure is shielded and therefore due to that a large torsion moment is induced on the structure. The gravity load on the structure is computed as the sum of the Jacket self-weight, the weight of top facilities and that of piles. The self-weigh of Jacket is distributed over the joints of structure proportionally. The weight of topside deck is distributed at four corner nodes of deck equally (see Table.1). The hydrodynamic forces consist of wave and current induced forces which are computed according to a modified form of Morison's equation (see for e.g. Chakrabarti, 1987, Emami et al, 2002) using a Stoke's 5^{th} order wave theory and a Wheeler stretching of current profile to the sea surface.

Table.1 Load Data for 4-Leg Jacket Platform

load	(MN)
selfweight of jacket	2.977
weight of topside deck	9.810
horizontal wave+current force	1.646
vertical wave+ current force	-0.552

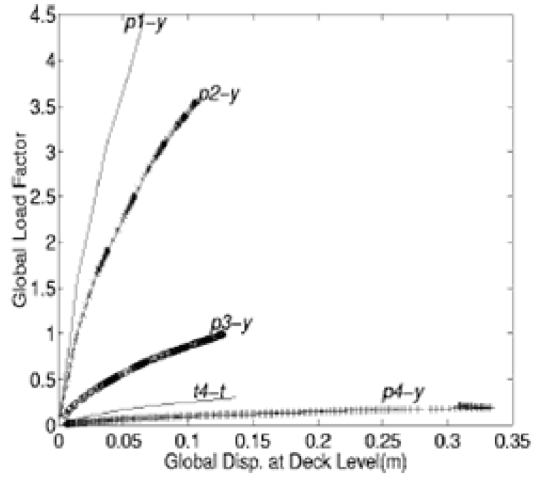

Fig.4 Static Response of 4-Leg Jacket Platform

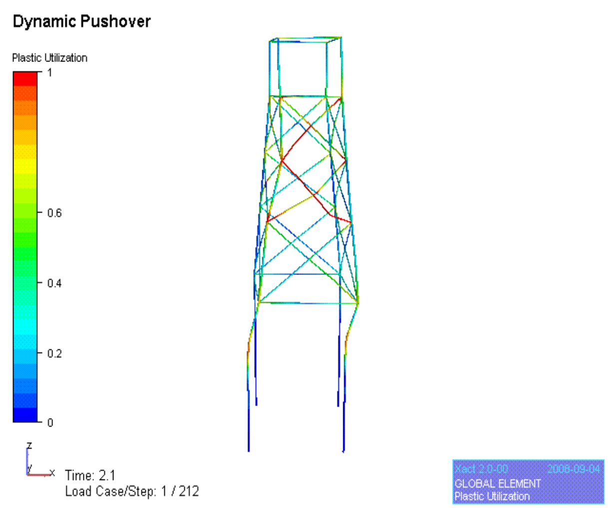

Fig.5 Deformed Model of 4-Leg Jacket-Pile-Soil system under Ship Impact at mid-node of El.340

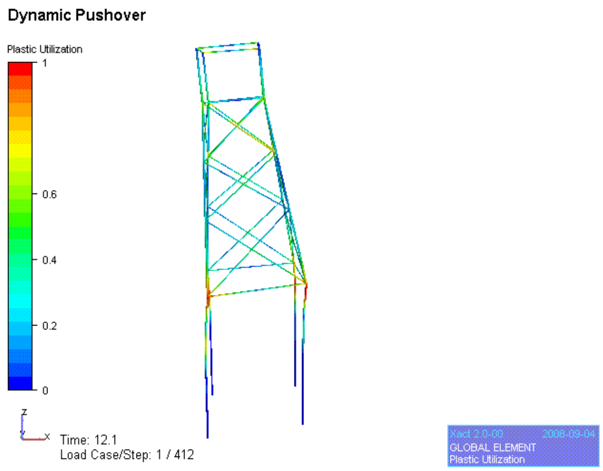

Fig.6 Deformed Model of 4-Leg Jacket-Pile-Soil system under Ship Impact at node.1 of El.335

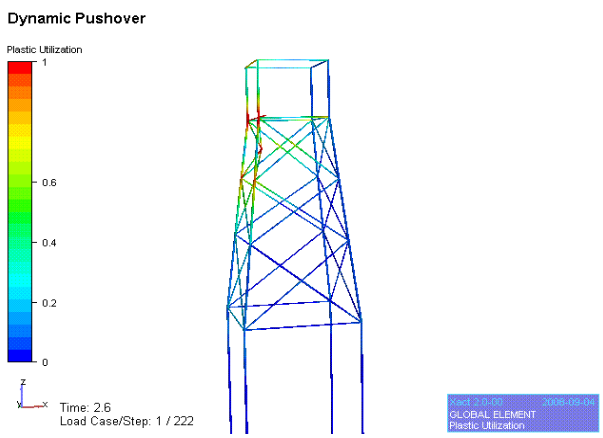

Fig.7 Deformed Model of 4-Leg Jacket-Pile-Soil system under Ship Impact at Mid-node of El.335

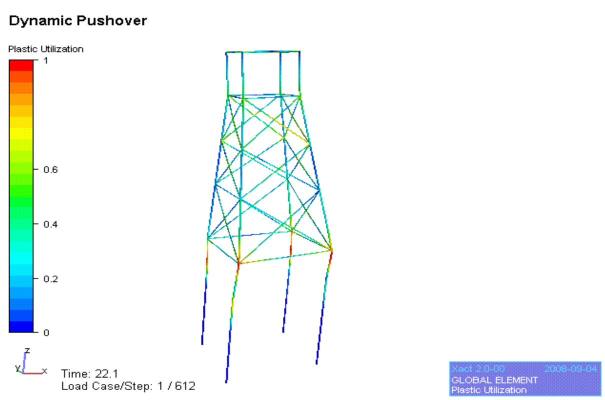

Fig.8 Deformed Model of 4-Leg Jacket-Pile-Soil system under Ship Impact at Node.2 of El.335

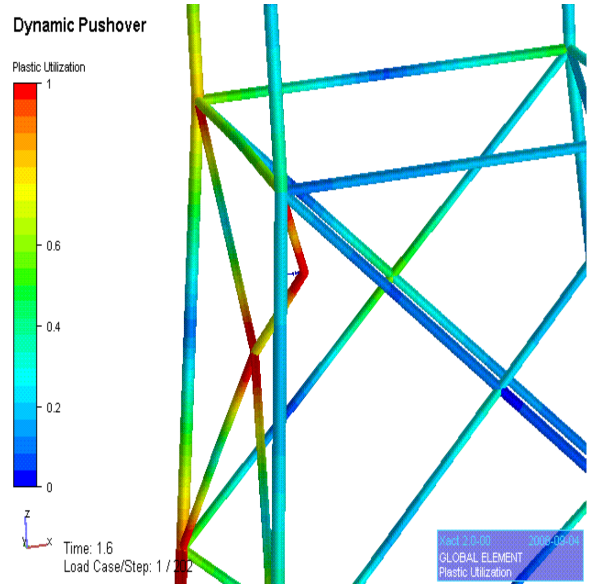

Fig.9 Zoomed View of Ship Impact at Mid-node of El.335 of 4-Leg Jacket-Pile-Soil System

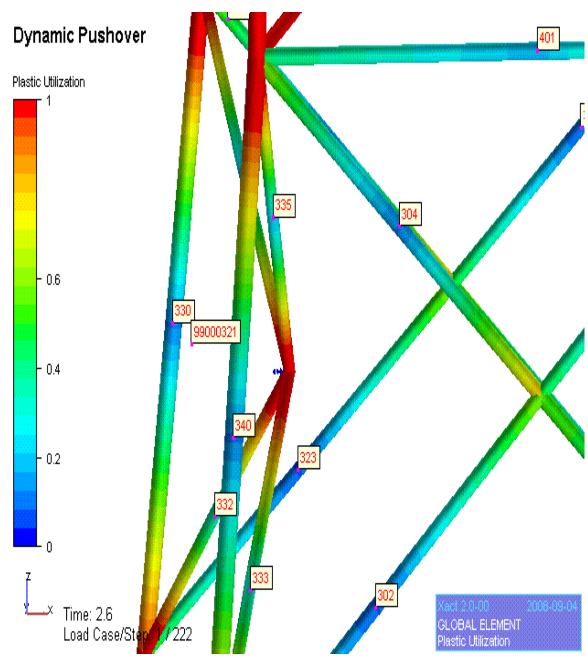

Fig.10 Zoomed View of Ship Impact at Node 2 of El.335 of 4-Leg Jacket-Pile-Soil System

3.1.4 Summary of Results

It is seen in Fig.4 that for lower values of lateral soil resistance (p4-y) the global load factor for the studied 4-leg jacket is more sensitive for the choice of torsional resistance of the pile-soil system. As seen, for the case of (p4-y) for which the lateral resistance of soil has been factored by 0.1 considering the corresponding torque-twist resistance (t4-t) has resulted in a quite significant increase of the overall system resistance and its stiffness. These synthetic curves might be the case when the pile is supported on a very loose saturated soil with very little lateral resistance and/or the case that the pile is end-bearing with short length while taking most its resistance from its tip resistance.

While increase of lateral soil resistance by a factor of 10.0 (p2-y) has resulted in a much stiffer global response but including (t2-t) for the same pile-soil system had no considerable change on the global jacket-pile-soil system response .The latter shows the coupling effects of (p-y) and (t-t) for the piles supported on relatively stiff soils against lateral movements. For the case of soil with increasing G with depth (p1-y), the global system response becomes stiffer than the three previous ones (p2-y), (p3-y) and (p4-y). It may be noted that only for the sake of this parametric study the (t-z) is not varied.

Fig.5 shows the deformed model and plastic interaction values of the 4-leg Malaysian Jacket-Pile-Soil system under a supply vessel impact at mid-node its main leg element no.340. Figs.6 to 8, show the deformed models for this jacket platform under supply ship collisions at nodes 1, 2 and mid-node of its bracing element 335, respectively. It can be seen that the hit main leg member has been damaged at its mid-node and completely dented in a scale 1:1 deformed model. However, the overall jacket-pile-soil system has been affected very significantly by this type impact. It is obvious that the overall deformation mode of jacket-pile-soil system is twist (torsion mode). A closer examination of the nodal displacements at nodes.110 and 120 at pile heads on the right hand side of the jacket platform indicated about 1.108m of difference in movement in global X-direction due to this kind of impact. This verified that under this type supply vessel impact, the supporting piles will sustain a significant lateral displacement. However, on the hit leg itself a rather considerable twist has also been observed during ship impact. The pile-soil torque-twist (t-t) mobilization curves in this case have also supported the presented our main idea

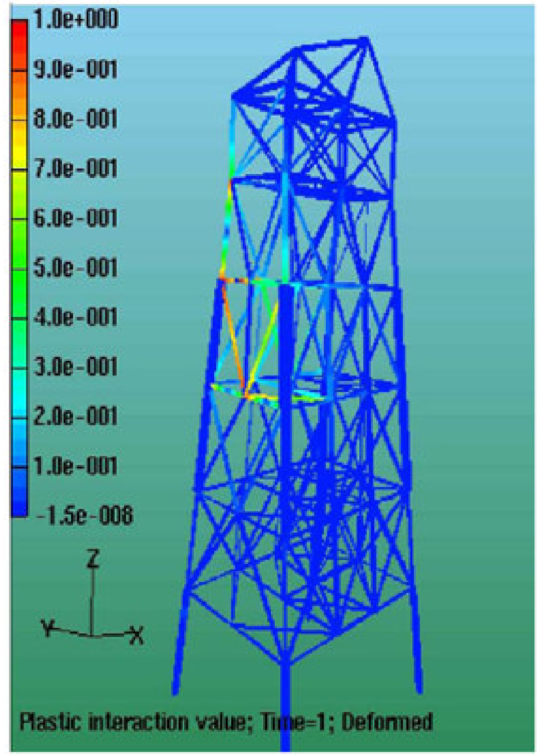

Fig.11 FE Model of 8-Leg Jacket-Pile-Soil System

in this article that the torque-twist pile-soil interaction behavior can not be neglected in all cases.

As seen, the impact at the mid-span of the bracing element 335 has resulted in a plastic hinge formation at this member at the hit point. However, the impact at the node 1 and in particular at 2 of this element has resulted in a significant overall deformation of the platform. On the other hand, the ship impact at the mid-node of the bracing element 335 has caused a significant twist in the main leg close to it. Figs.9 and 10 show the zoomed views of the deformed models of the jacket platform under the bracing impact modes. The spring elements at the impact point can be seen which model the ship-structure impact type which can be taken as elastic or in-elastic.

3.2 Case-2: An 8-leg North-Sea Jacket

3.2.1 Structural System

The finite element model of the 8-Leg Jacket structure used in this case study is shown in Fig.11. The structure consists of two longitudinal and four transverse frames. Longitudinal frames bracing system comprise mainly single diagonal braces and only X-braces at the first and the fifth storey.

Table.2 Wave Load Data for 8-Leg Jacket Platform

Water depth(d)	47.5m
100 year wave height(H_{100})	24.0m
Wave period(T_{100})	12.0sec
Current velocity(V_c)	0.7m/sec
Wave direction (α)	West-East
Drag coefficient(C_d)	0.77
Inertia coefficient(C_m)	2.0
Friction coefficient(C_x)	0.0001

The transverse frames have only K-braces. The supporting deck has been modeled as a truss and the topside facilities by a pyramid frame. The descriptions of structural and non-structural elements in detail are given in Emami (1998).

3.2.2 Foundation System

The foundation of the Jacket in this study is modeled as equivalent single piles penetrating into a depth of 28m below mud-line. Due to the relatively short length of the designed skirt piles in this case, they have been grouted at the bottom where the piles have penetrated into a sand layer.

Hence, the pile-tip is considered to be plugged to ensure the end-bearing resistance. Since the lateral resistance may be mobilized at the upper part of the soil, the designed pile condition is not modified and will be used in the first part of this study. The piles-soil interaction is modeled as non-linear disks as described above. The detail description of pile-soil is given in Emami (1998).

3.2.3 Load Description

The gravity, environmental and accidental loading are applied on the Jacket platform. The gravity load consists of self-weight of jacket, topside decks, piles and pile guides. The self-weight of jacket is applied on each element as distributed load and also the other parts are considered as equivalent nodal loads.

An accidental load is considered as the ship impact induced force on the horizontal bracing (element: 305) of the jacket platform as shown in Fig.11. The ship is considered to have a mass of 5000tons and a maximum speed of 2.0m/sec. The impact point on the horizontal bracing is taken to be the mid-span. Then in addition of lateral force a torsional moment is applied on the main leg element from simple structural mechanics theory.

3.2.4 Summary of Results

It can be seen in Fig.12 that the displacement response at node 101 in y-Direction during the initial phase (i.e. about impact duration) is almost the same for the Jacket platform with and without considering the torsional stiffness of the pile-soil system. While, the response curves of the two systems after this phase particularly after t=1.5sec show a tangible difference. The maximum displacement of node 101 in y-direction at time t=1.5sec for the Jacket-pile-soil system without considering (t-t) stiffness is about 0.022m while for the same system with having (t-t) effect is less than 0.012m.

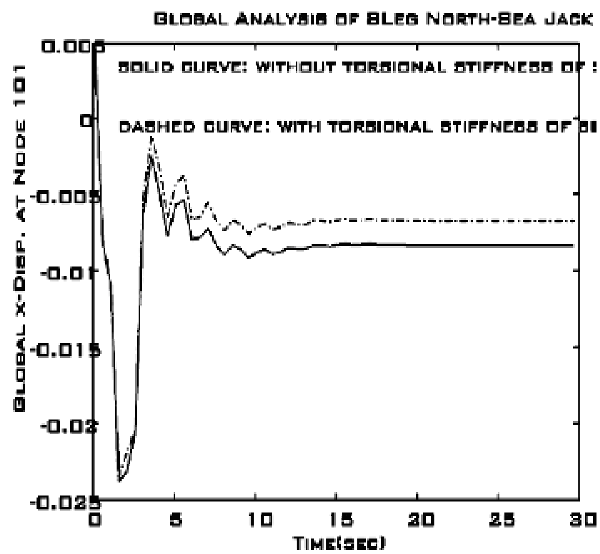

Fig.12 Dynamic Response of 8-Leg Jacket Platform at Node 101 in Global Y-Direction

This shows that considering (t-t) resistance has resulted in a much stiffer response (about 45% difference). At time after t=15sec the response curves of the platform with and without (t-t) effect become almost constant with magnitudes of about 0.028m and 0.022m (ab.21.4% difference).

It is observed in Fig.13 that the response at node 101 in global x-direction is almost the same for the jacket-pile-soil system with and without (t-t) effect until t=1.0sec but at time t=1.5sec a rather small difference about 0.001m is observed. Then at t=4sec the displacement response for system with torsion stiffness is about 0.015 stiffer than the system with no such stiffness. After time t=15sec the response curves are almost constant with ultimate displacements of about -0.0035m and -0.0025m, respectively. Similar trends are observed for the responses at node 301 in x and y-directions.

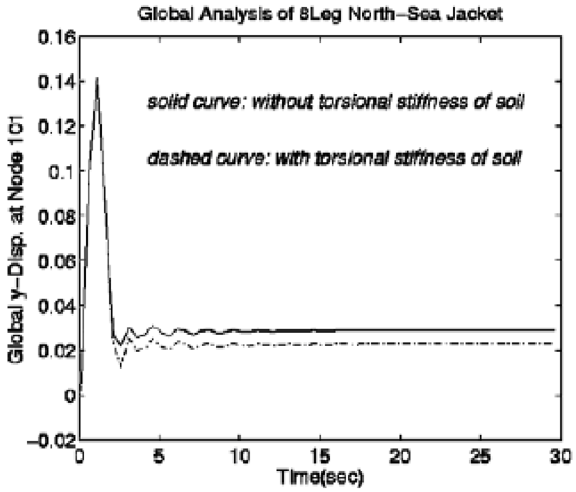

Fig.13 Dynamic Response of 8-Leg Jacket Platform at Node 101 in Global X-Direction

However, the maximum displacements at node 301 in global y-direction were about 0.07m (i.e. 33%) larger than the peak displacement at node 101. The peak displacement at node 301 in global x-direction was about -0.028m at time t=1.5sec compared to a peak value of -0.024m at node 101. After this point slight difference is observed. The ultimate displacement is about -0.0105m compared to the value -0.0095m (max. difference about 0.001m).

4 Conclusions

A rather simple torque-twist (t-t) model based on disk idealization of pile-soil interaction and simple continuum mechanics theory is developed similar to API's (t-z), (p-y) and (q-z) model. It is observed that for the case of 4-leg offshore Jacket platform the influence of soil torsional stiffness on the global system behavior is greatly dependent on the lateral pile-soil resistance. This means that there is a strong coupling between (p-y) and (t-t) is observed for the cases studied. It is also concluded that the pile-soil system response and its overall failure mode mainly depends on the type of ship impact on the structural members of the jacket platform. It is seen that soft impact mode on bracing members in most cases localizes the damage by formation of plastic hinges at the impact area and while the hard impact on the main leg member may induce an overall failure mode of jacket-pile-soil system. Mobilization of Pile-Soil and its failure mode hence could be affected by the type of dynamic impact or hydrodynamic loading on the jacket superstructure itself. It is also shown that for the case of 8-Leg Jacket platform the global dynamic response of the system under ship impact on a horizontal bracing is significantly influenced after initial phase (impact duration) by the choice of (t-t) for the studied case. This study showed that the effect of torsional behavior of pile-soil system could not be always neglected as often is assumed in the offshore industry.

References:

[1] API RP2A- LRFD (1993): “Planning, Design and Construction of Fixed Offshore Platforms, American Petroleum Institute, USA.

[2] Chakrabarti S.K. (1987):"Hydrodynamics of Offshore Structures, WIT. Press, UK.

[3] Emami Azadi, M.R. (1998): “Analysis of Static and Dynamic Pile-Soil-Jacket Behaviour”, Dr.ing. Thesis, NTNU, Norway.

[4] Emami Azadi, M.R. (2002): “Verification of Disk Pile-Soil Model”, Report PSPF-2002- TH, Internal Report for Marine Research Inst., Norway.

[5] Emami Azadi, M.R. and Moan T. (2002):" Influence of Wave-In-Deck Forces on the Reliability of Jacket-Pile-Soil System", Proc. of ICOPMAS 2002, Ramsar, Iran.

[6] Emami Azadi M.R., Holmaas T. (2005):"A new test version of usfos computer program", Norway.

[7] Grande, L. and Nordal, S. (1979): “Current Trends in the Safety of Offshore Structures”, Proc. of the 17th Int. OTC, USA.

[8] Lango, H.V.(1991): “Cyclic Shear Modulus of intact Clays”, Dr.ing Thesis, NTH, Norway.

[9] Manuel, A. N. and Gladys, C. D. (2002): “Equivalent or Virtual Fixity Depth of Lateral and Axially Loaded Piles”, On-Line Presentation, J. of Geotec.Eng, ASCE, USA.

[10] Moan T., Hellan, O. and Emami Azadi, M.R. (1997): “Non-linear Dynamic vs. Static Analysis of Jacket Systems for Ultimate Limit State Check”, Proc. of Marine Technology Conference, Edinbrough, UK.

[11] Nogami, T. and Konagai, K. (1989), “Time Domain Response of Dynamically Loaded Single Piles”, J. of Mech. Eng., ASCE, Vol.112, USA.

[12] Nordal, S., Grande, L. and Janbu, N.(1985), “ Prediction of Pile Behavior”, Div. of Geotechnical Eng. , Bul.15, NTH, Norway.

[13] Poulos, H.G. (1975): “Torsional Response of Piles”, J. of Geotechnical Eng., ASCE, Vol.101, USA.

[14] Przemieniecki R. (1968):"The Matrix Structural Analysis", Prentice-Hall New, York, USA.

[15] Randolph, M.F. (1982): “Piles Subjected to Torsion”, J. of Geotechnical Eng., ASCE, Vol.107, USA.

[16] Reddy J.N. (1985), :"An Introduction to the Finite Element Method", Mc-Graw Hill Company, New York, USA.
[17] Soreide T. and Amdahl J. (1986):"Usfos Computer Program for Ultimate Strength Analysis of Framed Offshore Structures", Theory Manual, Sintef, Norway.
[18] Stoll, U.W. (1976): “Torsional Response of Piles”, J. of Geotechnical Eng., ASCE, Vol.102, USA.
[19] Svano, G., Madshus, C. and Lango, H. (1993): “On the Validity of Non-linear Spring Idealization for Soil-Pile Interaction”, Proc. of Eurodyn '93, Trondheim, Norway.
[20] Wolf, J.P. and Meek, J.W. (1992): “Dynamic Response of Single Piles”, J. of Geotechnical Eng., Vol.120, USA
[21] Zienkiewicz, O.C. and Taylor R.L. (1989): "The Finite Element Method", Vol.1, Basic Formulation, Mc-Graw Hill Company, New York, USA.